International Journal of Mechanical, Industrial and Aerospace Sciences
ISSN: 2517-9950
Vol:11, No:7, 2017

# Nickel Electroplating in Post Supercritical $CO_2$ Mixed Watts Bath under Different Agitations

Chun-Ying Lee, Kun-Hsien Lee, Bor-Wei Wang

***Abstract*—**The process of post-supercritical $CO_2$ electroplating uses the electrolyte solution after being mixed with supercritical $CO_2$ and released to atmospheric pressure. It utilizes the microbubbles that form when oversaturated $CO_2$ in the electrolyte returns to gaseous state, which gives the similar effect of pulsed electroplating. Under atmospheric pressure, the $CO_2$ bubbles gradually diffuse. Therefore, the introduction of ultrasound and/or other agitation can potentially excite the $CO_2$ microbubbles to achieve an electroplated surface of even higher quality. In this study, during the electroplating process, three different modes of agitation: magnetic stirrer agitation, ultrasonic agitation and a combined mode (magnetic + ultrasonic) were applied, respectively, in order to obtain an optimal surface morphology and mechanical properties for the electroplated Ni coating. It is found that the combined agitation mode at a current density of 40 A/dm$^2$ achieved the smallest grain size, lower surface roughness, and produced an electroplated Ni layer that achieved hardness of 320 HV, much higher when compared with conventional method, which were usually in the range of 160 to 300 HV. However, at the same time, the electroplating with combined agitation developed a higher internal stress of 320 MPa due to the lower current efficiency of the process and finer grain in the coating. Moreover, a new control methodology for tailoring the coating's mechanical property through its thickness was demonstrated by the timely introduction of ultrasonic agitation during the electroplating process with post supercritical $CO_2$ mixed electrolyte.

***Keywords*—**Nickel electroplating, micro-bubbles, supercritical carbon dioxide, ultrasonic agitation, magnetic stirring.

## I. Introduction

DUE to its beneficial effects on the plating of metallic coatings, such as nickel, copper, zinc and chromium etc., sonoelectrodeposition has been proposed extensively in the literature. The dilatation and compression of the acoustic wave in the electrolyte renders the formation and collapse of microbubbles, and generates shock waves accordingly. Thus, the enhanced agitation increases the diffusion of the ionic species [1] and interacts with the nucleation process during deposition. Refined grains are obtained in the coatings [2]. Moreover, the cavitation and jet flow generated in ultrasonic excitation can help to disperse the aggregates in the electrolyte and to improve the surface quality and uniformity of deposition [3]. Therefore, ultrasonic excitation can be employed in the control of agitation in the electrolyte. Dini and Johnson [4] reported that, in the electroplating with nickel sulphamate bath, ultrasonic agitation reduced the defects caused by the incorporated impurity. In Watts bath, Vasudevan et al. [5] discovered that the limit current density and deposition rate could be raised by applying ultrasonic excitation at 22 kHz. In the other words, the side reaction of hydrogen reduction was successfully suppressed by the ultrasonic agitation. Regarding the mechanical property of the coating plated under the assistance of ultrasonic excitation, Prasad et al. [6] reported the increase in surface smoothness, hardness, wear resistance and fatigue performance. However, Kobayashi et al. [7] revealed the ultrasonic agitation could change the deposition texture of nickel from (111) to (200) and decrease the deposition rate. The ablation and erosion on cathode induced from the cavitation and jet flow in ultrasonic excitation and the re-dissolution of the removed debris was considered to be main mechanism in this finding. Therefore, not all positive conclusions regarding the ultrasonic agitation were reported.

In the electrodeposition of metallic coating, a supercritical $CO_2$ emulsion electrolyte was introduced by Yoshida et al. [8]. The property of high diffusivity and low viscosity of the supercritical $CO_2$ mixed electrolyte makes the obtained nickel coating with greatly improved surface finish [9], [10], higher hardness [11]-[13], and better corrosion resistance [14], but higher internal stress [15], [16]. Although high quality coating with nearly no void was obtained, the requirement of high pressure environment in the process can be a costly constraint for the application in workpieces with large dimensions. In seeking an alternative for investing the high-cost large-sized pressure chamber, Nguyen et al. proposed a post-supercritical $CO_2$ assisted deposition process [17]. The mixing of electrolyte with supercritical $CO_2$ was still carried out inside a high pressure chamber. However, the deposition process was conducted in atmospheric environment with the de-pressurized electrolyte which can mix with the other conventional electrolyte. The oversaturated $CO_2$ which was dissolved in its supercritical state started to form microbubbles and escape from the electrolyte. These microbubbles assumed the similar function as in the supercritical $CO_2$ assisted process, and similar improvement in coating property was obtained.

In spite of the beneficial effect from the microbubbles evolved in the post-supercritical $CO_2$ assisted process, the remained amount of oversaturated $CO_2$ in the electrolyte decreases with elapsed time. Furthermore, the condition of agitation in electrolyte also affects the escape of microbubbles. Therefore, controlling the ultrasonic agitation in the post-supercritical $CO_2$ assisted process can adjust the formation of microbubbles in the electrolyte and tailor the coating's

C. Y. Lee is with the Department of Mechanical Engineering, National Taipei University of Technology, Taipei 10608, Taiwan (corresponding author, phone: 886-2-87731614; fax: 886-2-27317191; e-mail: leech@ ntut.edu.tw).
K. H. Lee is with the Graduate Institute of Mechatronic Engineering, National Taipei University of Technology, Taipei 10608, Taiwan.
B. W. Wang is with the Graduate Institute of Manufacturing Technology, National Taipei University of Technology, Taipei 10608, Taiwan.

property. In this study, the effects of applying different agitations in different power and timing on the electroplating of nickel during a post-supercritical $CO_2$ assisted process were investigated. Both the formation of microbubbles and the conventional effect of ultrasonic excitation were examined.

## II. Experimental

A Watts bath was employed in the electroplating of nickel. Table I shows the compositions of the electrolyte. A strip of 20 mm×25 mm×5 mm nickel with purity greater than 99.9% served as the anode which size was larger than that of cathode to have uniform electric field distribution over the cathode. This anode was brushed first to remove the oxide on the surface, then washed with de-ionized water in an ultrasonic cleaner. A 0.5-mm thick brass plate was cut using CNC electrical discharge machine to obtain a 2.2 $mm^2$ circular cathode. The circular shape was chosen to minimize the uneven electric field distribution around corners.

TABLE I
Compositions of the Watts Electrolyte

| Ingredients | Concentration (g/L) |
|---|---|
| $NiSO_4 \cdot 6H_2O$ | 300 |
| $NiCl_2 \cdot 6H_2O$ | 50 |
| $H_3BO_3$ | 30 |

Table II presents the process parameters used in the mixing and electroplating of this study. For the post supercritical $CO_2$ assisted electroplating, three different agitation modes at different current densities were investigated. Moreover, the power effect of the ultrasonic agitation was also examined by adjusting the voltage applied to the agitator. The specifications of the ultrasonic agitator used in this study are listed in Table III (Whirl Best International Company). The adjustment on the voltage only changed the power of the ultrasound with the frequency fixed at 40 kHz.

After the completion of electroplating, the weight gain of the specimen was measured by a precision balance, and the current efficiency was calculated using Faraday's law accordingly. The surface roughness of the coating was measured with an α-step profilometer (KOSAKA Surfcorder SEF3500), while the surface morphology was examined with a scanning electron microscope (JEOL JSM-7401F). An X-ray diffractometer (MAC Science M03XHF) was employed to measure the crystalline microstructure of the coating. Subsequently, the effective grain size was calculated from the full-width-at-half-maximum (FWHM) of the diffraction peaks by using the Scherrer's equation. For the mechanical properties of the coating, the hardness of the coating was measured with micro-Vickers hardness tester (Mitutoyo – Akashi, MVK-G1000) at 25-g loading of 10-s duration. The deposition stress of the coating was determined by measuring the bending curvature of a strip specimen and using the Stoney's equation.

TABLE II
Parameters Used in Electroplating Process

| Parameter | Sc-$CO_2$ mixing | Post Sc-$CO_2$ electroplating |
|---|---|---|
| Temperature, °C | 50 | 50 |
| Pressure, MPa | 13.8 | 0.1 |
| Speed of magnetic stirrer, rpm | 500 | 400 |
| Agitation Mode | Magnetic | Magnetic, Ultrasonic, Magnetic & Ultrasonic |
| Current density, A/$dm^2$ | – | 5 - 40 |
| Voltage to Ultrasonic Agitator, V | – | 30 |

TABLE III
The Specifications of the Ultrasonic Agitator Used in This Study

| Item | Specifications |
|---|---|
| Model No. | WB4038-45LB |
| Resonance frequency (kHz) | 40±0.5 |
| Resonance impedance (Ω) | ≤ 25 |
| Static capacitance (pF) | 3800 pF±10% |
| Maximum power (W) | 50 |
| Maximum temperature (°C) | 100 |

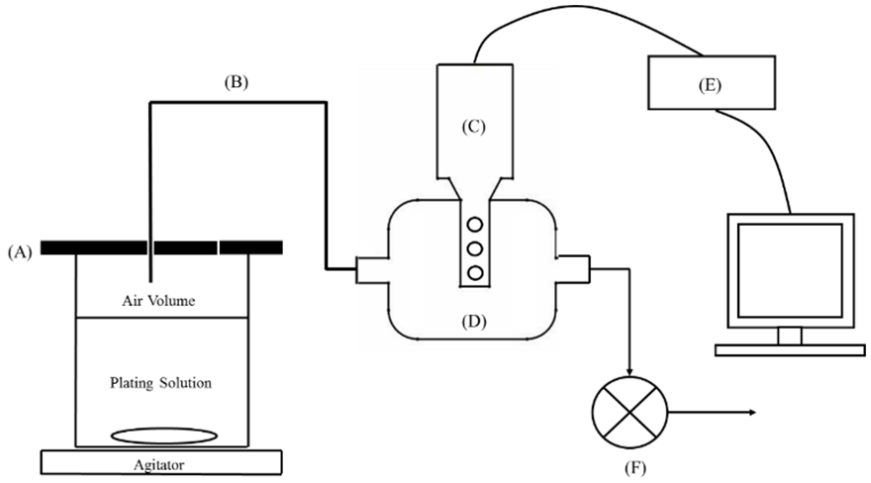


Fig. 1 The schematic diagram of the setup for measuring the release of $CO_2$ from the post supercritical $CO_2$ mixed electrolyte: (A) acrylic cover, (B) 8-mm diameter rubber tube, (C) $CO_2$ detector (Paspont $CO_2$ Sensor ps-2100), (D) measurement chamber, (E) data acquisition module PS-2009, (F) air pump

In order to understand the release of oversaturated $CO_2$ from the post supercritical $CO_2$ mixed electrolyte, an experimental setup as shown schematically in Fig. 1 was established. The plating solution in a beaker was contained with an acrylic cover. One of the ventilation holes on the cover was connected to a measurement chamber via a rubber tube, the other served as the ventilation for air intake. Inside the measurement chamber, a $CO_2$ sensor monitored the $CO_2$ concentration, while an air pump kept extracting gas from the chamber. The measured $CO_2$ concentration was acquired by the data acquisition module and stores in a personal computer. Thus, the variation of the $CO_2$ release over time from the plating solution can be recorded.

## III. Results and Discussion

### *A. The Release of Oversaturated $CO_2$ from the Post Supercritical $CO_2$ Mixed Electrolyte*

Since the $CO_2$ microbubbles were considered to be the main beneficial contributor to the process improvement in supercritical $CO_2$ assisted process, the understanding of its release from the electrolyte was crucial for the process control. Fig. 2 presents the time variation of the released $CO_2$ concentration for three different agitation modes. For the electrolyte under only magnetic stirrer agitation, gas bubbles with overall rotation inside the electrolyte caused a rather fast release of $CO_2$ during the first 5 min. On the contrary, ultrasonic agitation only caused fine bubbles to appear near the ultrasonic hone. This localized agitation slowed the release of $CO_2$ from the electrolyte comparing with its magnetic counterpart. With the combined agitation from ultrasound and magnetic stirrer, a drastic increase in the release rate was observed at the beginning of agitation. This was resulted from the combined motion of local ultrasonic excitation and the magnetic stirring induced global flow. However, because of the constant total amount of dissolved $CO_2$ in the electrolyte during supercritical mixing, the faster the release rate, the shorter the release duration. It is realized from Fig. 2 that the post supercritical effect should decrease with time and could last for first 15 min.

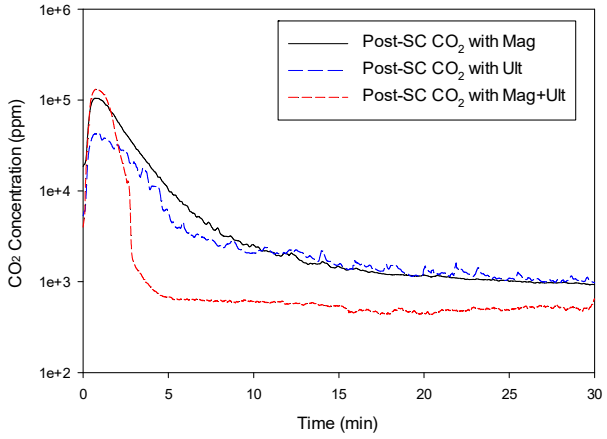


Fig. 2 The release of $CO_2$ from the supercritical $CO_2$ mixed electrolyte under three different agitation modes, respectively

### *B. The Electrodeposition for Different Processes and Agitations*

Fig. 3 presents the current efficiency of the Ni plating at different current densities and for different processes. Basically, for the current density studied (5 – 40 ASD), the current efficiency decreased gradually as the current density increased. The difference between those of conventional and post supercritical $CO_2$ processes enlarged as the current density was raised. The microbubbles in the electrolyte decreased its conductivity, and consequently, the current efficiency. Moreover, the combined agitation of ultrasound and magnetic stirrer well mixed the electrolyte and decreased the thickness of diffusion layer. This enhanced agitation reduced the reduction of hydrogen during electroplating and improved the current efficiency for conventional process. However, for the post supercritical $CO_2$ process, the well mixing denoted more microbubbles stayed around the cathode and facilitated the removal of hydrogen from its reduction site. Therefore, the enhanced hydrogen reduction decreased the current efficiency.

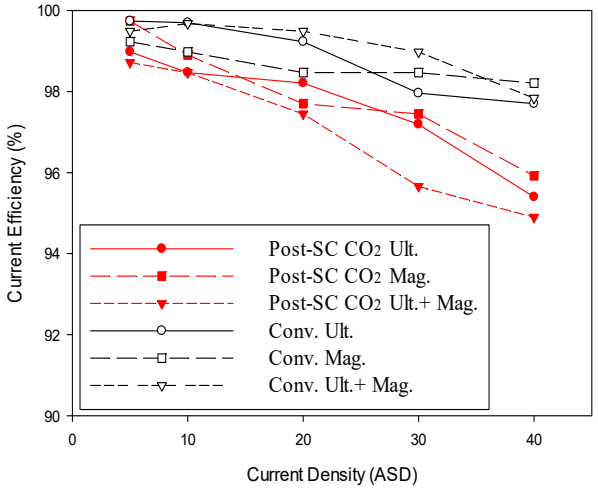


Fig. 3 Current efficiency of the deposition at different current densities for different deposition processes and agitations

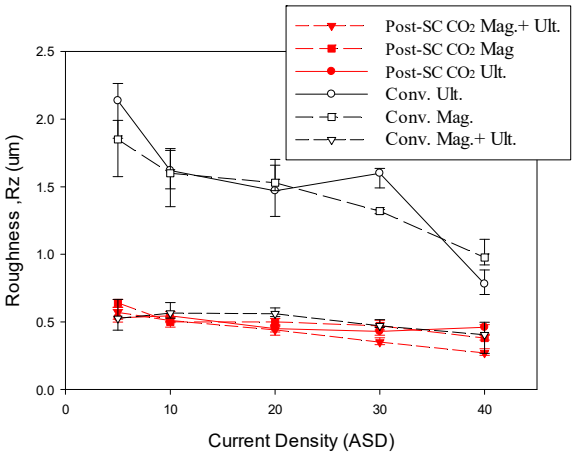


Fig. 4 Surface roughness of the coating plated at different current densities for different deposition processes and agitations

The surface roughness of the resulted coatings is shown in Fig. 4. It is seen that the roughness of the conventional process with either ultrasound or magnetic stirring decreased with the raise of current density in electrodeposition. However, they were much larger than the coating plated with combined agitation or the post supercritical $CO_2$ counterparts. The raise of current density usually refines the grains and smoothens the coating's surface. Moreover, the post supercritical $CO_2$ process inherited the characteristics of its supercritical counterpart as expected. Fig. 5 presents the SEM surface morphology of the coatings plated under combined agitation and different current densities. A nodular morphology was seen for all current densities, and little change was observed with the variation of current density as that from the roughness measurement in Fig. 4.

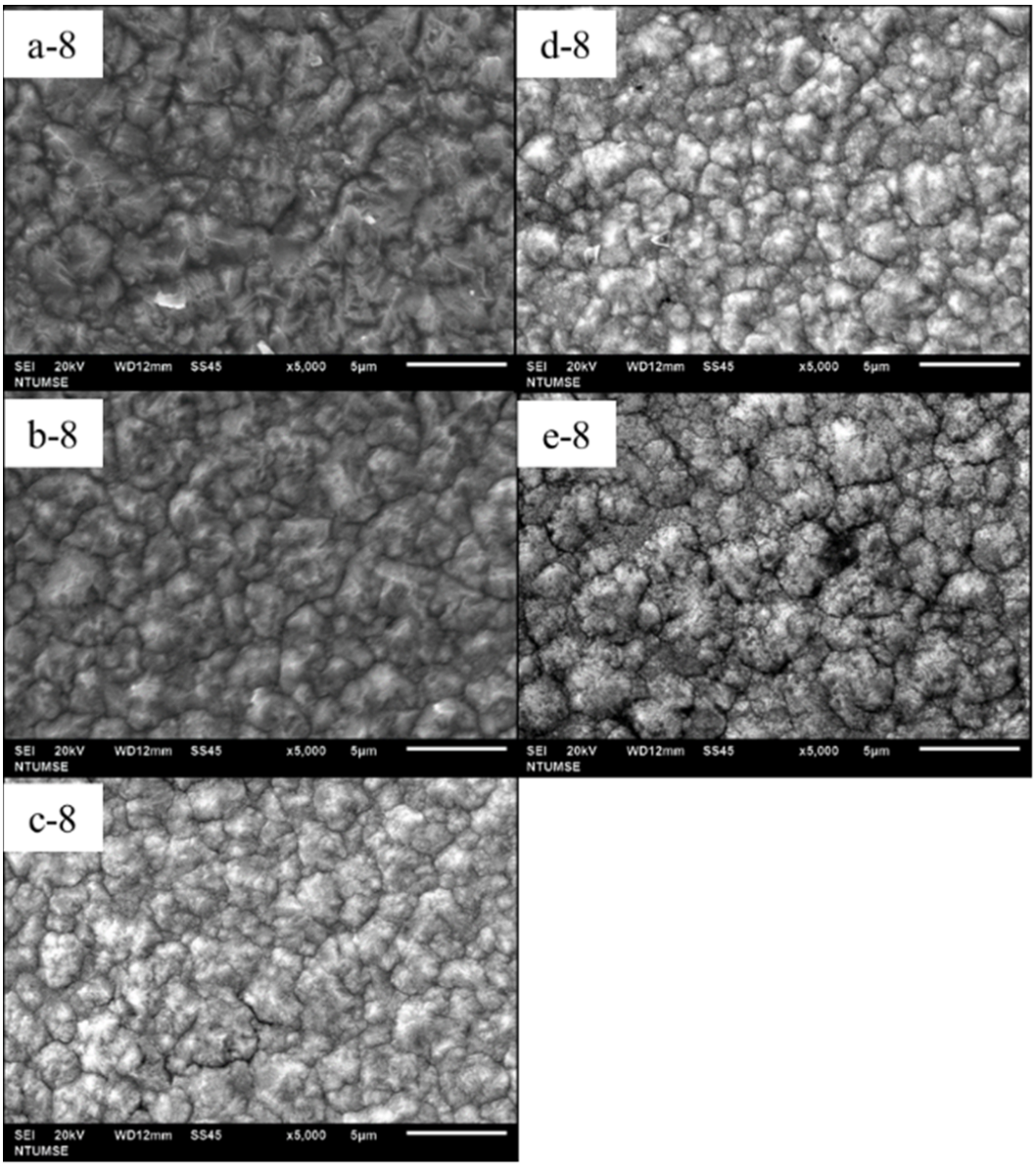


Fig. 5 SEM photomicrographs of the coatings plated under combined agitation and different current densities: (a-8) 5 A/dm$^2$, (b-8) 10 A/dm$^2$, (c-8) 20 A/dm$^2$, (d-8) 30 A/dm$^2$, (e-8) 40 A/dm$^2$

*C. The Microstructure and Mechanical Properties*

Since the X-ray diffraction spectra did not show much difference among all prepared coatings, the results were not presented. However, for the coatings prepared using post supercritical $CO_2$ process with different agitation modes, the corresponding grain size obtained from the diffraction peak by employing Scherrer's equation was calculated and shown in Fig. 6. The coating prepared from the combined agitation showed the most refined grain at high current density. At low current density, the coating took longer time duration to reach

the required thickness. As seen in Fig. 2, the release of oversaturated $CO_2$ bubbles was so fast for the combined agitation mode that the depletion in releasing the $CO_2$ bubbles reached at early state. Thus, the top layer of the coating was deposited with barely the post supercritical $CO_2$ effect. It should be the reason that larger grains than those from ultrasonic agitation alone were measured.

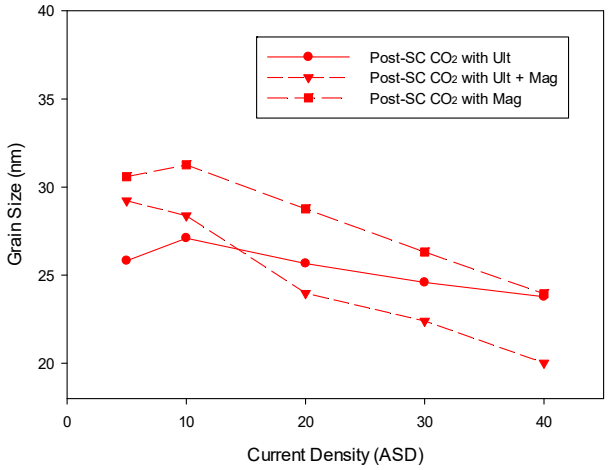


Fig. 6 The grain size of the coating prepared from the post supercritical $CO_2$ process with different current densities and agitation modes

Fig. 7 presents the variation of hardness through its thickness for the coating prepared at 40 A/dm$^2$ and post supercritical $CO_2$ processes with different agitation modes. For all three agitation modes in post supercritical $CO_2$ process, the hardness decreased as the coating grew thicker. It is realized that, from the $CO_2$ bubble release rate shown in Fig. 2, the post supercritical $CO_2$ effect diminished with elapsed time. Therefore, the decrease in coating's hardness with thickness can be expected. Moreover, the combined agitation can release the oversaturated $CO_2$ microbubbles more quickly at the beginning of the deposition, more pronounced effect in hardness increment is seen. However, as explained previously, the quicker release rate drops the level of continuous bubble dissolution in shorter time span. It is thus seen the hardness dipped faster with the increase in coating's thickness.

For comparing the hardness of the coatings prepared with different processes, current densities and agitation modes, Fig. 8 presents those measured at 20 μm from the substrate interface. The trend of increasing hardness with deposition current density was observed in Fig. 8. It is also seen that post supercritical $CO_2$ process prepared the coating with slightly higher hardness than its conventional counterpart. In the other words, within 20 μm range, the post supercritical $CO_2$ effect still prevailed. At low current density, e.g. 5 ASD, the coating from conventional plating had low hardness, and the hardness enhancement from post supercritical $CO_2$ process was more dominant. Overall speaking, the post supercritical $CO_2$ process with combined agitation still demonstrated the highest hardness performance.

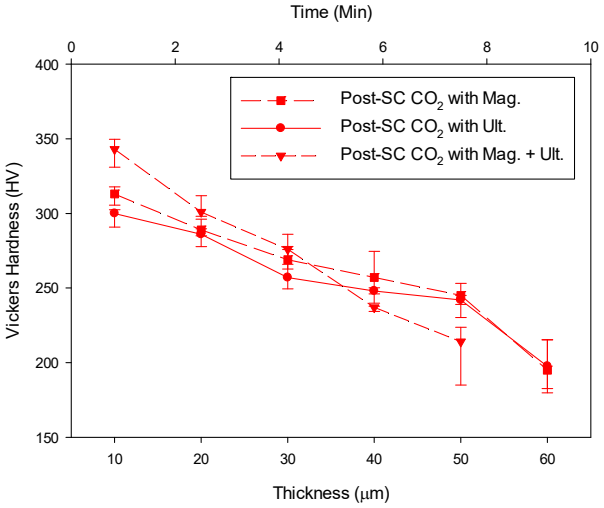


Fig. 7 The variation of hardness through its thickness for the coating prepared at 40 A/dm$^2$ and post supercritical $CO_2$ processes with different agitation modes

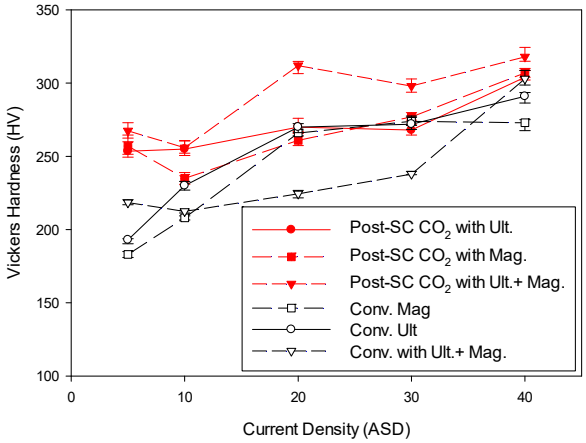


Fig. 8 The hardness at 20 μm from the substrate interface for the coating prepared with different processes, current densities, and agitation modes

The internal stress of the coating usually controls the dimensional stability of workpiece after deposition, especially when thick coating is prepared. Moreover, from our previous study, the internal stress is more prominent in supercritical $CO_2$ electroplating than its conventional counterpart [17]. Thus, only the internal stresses of the coating prepared from post supercritical $CO_2$ process with different agitation modes are presented in Fig. 9. From the results shown in Fig. 9, it is noted that the internal stress increased with the raise of current density for all three different agitation modes. By referring to the results shown in Fig. 2, the current efficiency decreased with the current density. More hydrogen reduction accompanied the nickel deposition should more or less increased the inclusion of hydrogen bubbles into the coating. Therefore, more tensile internal stress developed in the coating [16], [18]. Among the three agitation modes, the one with ultrasonic agitation prepared the coating with higher internal

stress. As mentioned earlier, the ultrasonic agitation only excited the local $CO_2$ microbubbles. The global movement of the electrolyte was limited. Therefore, more hydrogen encapsulation in the coating could be possible cause for the higher internal stress observed. Although the coating prepared with combined agitation showed low internal stress at low current density, the internal stress quickly picked up at high current density. This should be related to the low current efficiency measured at high current density, as seen in Fig. 2. Both the more grain refinement and hydrogen reduction should be responsible for this result.

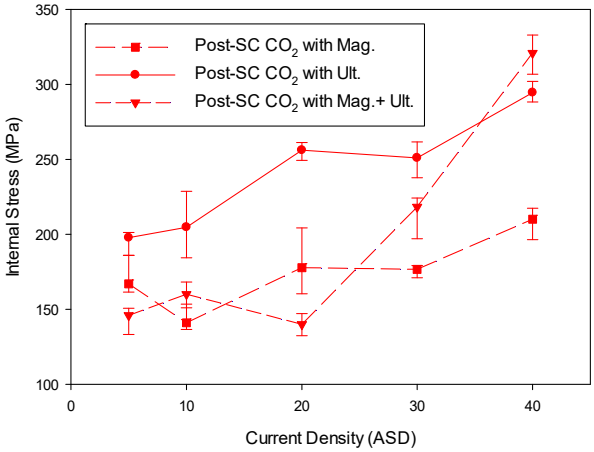


Fig. 9 The internal stress of the coating prepared at different current densities with different agitation modes in post supercritical $CO_2$ process

### *D.Approach for Tailoring Coating's Property via Agitation Control*

In order to demonstrate the controllability on the release of oversaturated $CO_2$ in the electrolyte after post supercritical $CO_2$ mixing and its influence on the mechanical property of the prepared coating, the electroplating was started with two different timings for agitation, respectively. One started the ultrasonic agitation 30 s after the electroplating under magnetic stirring, the other 2 min. As expected, starting the ultrasonic agitation earlier could release the oversaturated $CO_2$ from the electrolyte in the earlier phase of electroplating. However, the high volume of microbubbles released in the early phase reduced its available influence duration because of the constant total oversaturated $CO_2$ contained in the electrolyte. Triggering the more intensive release of $CO_2$ by ultrasonic agitation at later phase could prolong the influence of $CO_2$ microbubbles during electroplating. The hardness distribution measurements of the coatings prepared from these two controlled agitation modes are shown in Fig. 10. Apparently, the earlier introduction of the ultrasonic agitation gave the higher hardness of the coating at the beginning. But, this enhanced hardness trailed that from the coating prepared with delayed introduction of ultrasonic agitation at larger thickness. This example shows the possibility of using controlled ultrasonic agitation to tailor the coating's property over the course of post supercritical $CO_2$ assisted electroplating.

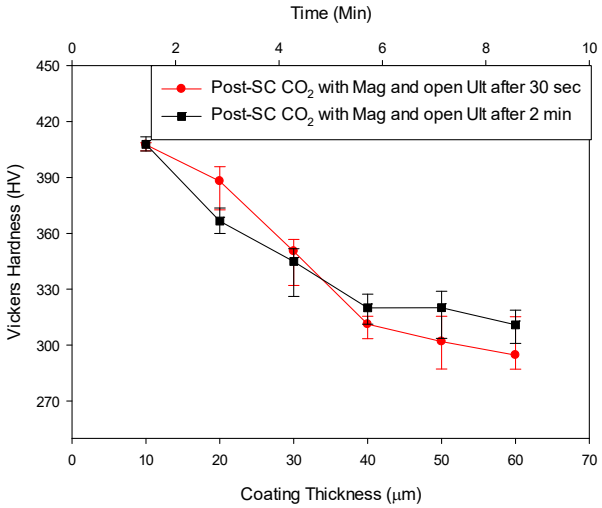


Fig. 10 The through-the-thickness hardness profiles for the coatings prepared from post supercritical $CO_2$ assisted electroplating process with ultrasonic agitation being introduced at two different stages, respectively

## IV. Conclusion

The electroplating from post supercritical $CO_2$ assisted process in Watts bath was shown to prepare the nickel coating with higher hardness, finer grain, smoother surface, and higher internal stress than from its conventional counterparts. In this study, more controllability on this post supercritical effect was proposed using ultrasonic agitation and the current density during the course of electroplating. Because of the constraint in total amount of oversaturated $CO_2$ in the supercritical mixing with electrolyte, electroplating with high current density and subsequently short time duration showed more beneficial effect from the release of microbubbles. However, the adequate increase in current density was still limited by the decreasing in current efficiency of electroplating. The combined agitation of magnetic stirrer and ultrasonic excitation was able to drastically increase the release of oversaturated $CO_2$ microbubbles from the electrolyte and to obtain the characteristics from supercritical electroplating. Moreover, the timely introduction of ultrasonic agitation during the electroplating process with post supercritical $CO_2$ mixed electrolyte was shown to offer a new control methodology for tailoring the coating's mechanical property through its thickness.

## Acknowledgment

The financial support from Ministry of Science and Technology, Taiwan, under Grant No. MOST 104-2221-E-027-110 is gratefully acknowledged.

## References

[1] S. A. Perusich, and R. C. Alkire, "Ultrasonically Induced Cavitation Studies of Electrochemical Passivity and Transport Mechanisms," *Electrochemical Society*, vol. 138, no. 3, 1991, pp. 700-707.
[2] M. E. Hyde, and R. G. Compton, "How Ultrasound Influences the Electrodeposition of Metals," *Electroanalytical Chemistry*, vol. 531, no. 6, 2002, pp. 19-24.

[3] C. T. Walker, and R. Walker, "Effect of Ultrasonic Agitation on Some Properties of Electrodeposits," *Electrodeposition and Surface Treatment*, vol. 1, no. 6, 1973, pp. 457-469.
[4] D. W. Dini, and H. R. Johnson, "The Influence of Nickel Sulfamate Operating Parameters on the Impurity Content and Properties of Electrodeposits," *Thin Solid Films*, 1978, vol. 54, no. 2, pp. 183-188.
[5] R. Vasudevan, R. Devanathan, K. G. Chidambaram, "Effect of Ultrasonic Agitation During Electroplating of Nickel and Copper at Room Temperature," *Metal Finishing*, vol. 90, 1992, pp. 23-26.
[6] P. B. S. N. V. Prasad, R. Vasudevan, S. K. Seshadri, "The Effect of Ultrasonic Vibration on Nickel Electrodeposition," *Materials Letters*, vol. 17, 1993, pp. 357-359.
[7] K. Kobayashi, A. Chiba, N. Minami, "Effect of Ultrasound on Both Electrolyte and Electroless Nickel Depositions," *Ultrasonics*, vol. 38, 2000, pp. 676-681.
[8] H. Yoshida, M. Sone, A. Mizushima, K. Abe, X. T. Tao, S. Ichihara, S. Miyata, "Electroplating of Nanostructured Nickel in Emulsion of Supercritical Carbon Dioxide in Electrolyte Solution," *Chemistry Letters*, vol. 11, 2002, pp. 1086.
[9] H. Yoshida, M. Sone, A. Mizushima, H. Yan, H. Wakabayashi, K. Abe, X. T. Tao, S. Ichihara, S. Miyata, "Application of Emulsion of Dense Carbon Dioxide in Electroplating Solution with Nonionic Surfactants for Nickel Electroplating," *Surface and Coatings Technology*, vol. 173, 2003, pp. 285-292.
[10] T. F. M. Chang, M. Sone, A. Shibata, C. Ishiyama, Y. Higo, "Bright Nickel Film Deposited by Supercritical Carbon Dioxide Emulsion Using Additive-free Watts Bath," *Electrochimica Acta*, vol.55, 2010, pp. 6469-6475.
[11] H. Yan, M. Sone, A. Mizushima, T. Nagai, K. Abe, S. Ichihara, S. Miyata, "Electroplating in $CO_2$-in-Water and Water-in-$CO_2$ Emulsions Using a Nickel Electroplating Solution with Anionic Fluorinated Surfactant," *Surface & Coatings Technology*, vol. 187, 2004, pp.86-92.
[12] M. S. Kim, J. Y. Kim, C. K. Kim, N. K. Kim, "Study on the Effect of Temperature and Pressure on Nickel-electroplating Characteristics in Supercritical $CO_2$," *Chemosphere*, vol. 58, 2005, pp. 459-465.
[13] T. F. M. Chang, M. Sone, "Function and Mechanism of Supercritical Carbon Dioxide Emulsified Electrolyte in Nickel Electroplating Reaction," *Surface & Coatings Technology*, vol. 205, 2011, pp. 3890-3899.
[14] S. T. Chung, H. C. Huang, S. J. Pan, W. T. Tsai, P. Y. Lee, C. H. Yang, , and M. B. Wu, "Material characterization and corrosion performance of nickel electroplated in supercritical $CO_2$ fluid," *Corrosion Science*, Vol. 50, No. 9, 2008, pp. 2614-2619.
[15] C. V. Nguyen, C. Y. Lee, F. J. Chen, C. S. Lin, T. Y. Liu, "Study on the Internal Stress of Nickel Coating Electrodeposited in an Electrolyte Mixed with Supercritical Carbon Dioxide," *Surface & Coating Technology*, vol. 206, 2012, pp. 3201-3207.
[16] C. V. Nguyen, C. Y. Lee, L. Chang, F. J. Chen, C. S. Lin, "The Relationship Between Nano Crystallite Structure and Internal Stress in Ni Electrodeposited Films Pated by the Supercritical $CO_2$ Method," *Journal of The Electrochemical Society*, vol. 159, 2012, pp. 393-399.
[17] C. V. Nguyen, C. Y. Lee, F. J. Chen, C. S. Lin, L. Chang, 2013, "An Electroplating Technique using the Post Supercritical Carbon Dioxide Mixed Electrolyte," *Surface & Coatings Technology*, 232, pp.234-239.
[18] R. Weil, "The Origins of Stress in Electrodeposits, Review of the Literature Dealing with Stress in Electrodeposited Metal", *Plating*, vol. 58, 1971, pp. 137-146.